Aerosol and Air Quality Research, 14: 1443–1454, 2014

ISSN: 1680-8584 print / 2071-1409 online
doi: 10.4209/aaqr.2013.05.0168

Novel Technique for Profiling of Aerosol, Ozone and Water Vapor during Winter Using Mobile Radiometers over a Hilltop Station

Panuganti China Sattilingam Devara*, Sunil Manohar Sonbawne, Sanjoy Kumar Saha

Indian Institute of Tropical Meteorology, Dr. Homi Bhabha Road, Pune 411008, India

ABSTRACT

Following a novel approach, the vertical distributions of columnar aerosol optical depth (AOD), precipitable water content (PWC) and ozone (TCO) have been determined using compact, multi-filter, solar radiometers during winter period of 2002–2003. These profiles were obtained by making measurements at different altitudes while ascending to/descending from a rural site, elevated up to an altitude of about 1450 m above mean sea level (AMSL). Besides the wavelength dependency, the profiles depict significant layer structures which are explained on the basis of concurrent atmospheric stability parameters. The aerosol size distributions which were obtained from the inversion of spectral dependence of AOD at different altitudes show a mixture of power-law, mono- and bi-model distributions indicating the influence of aerosols originating from both anthropogenic and natural sources. The present results, representing a rural high-altitude station, are compared with those reported over a few selected similar high-altitude stations in North India, and also observed at a nearby urban station (Pune) in Central India to infer modulation of terrain-induced meteorological parameters on aerosol source strength. The importance of the experimental approach and profiles of AOD and pre-cursor gases over areas with scarce alternative measurements, networks with sporadic presence of ground sites and limited number of satellite retrievals is highlighted.

Keywords: Aerosols; Ozone; Water vapor; Remote sensing; High-altitude station; ABL; Winter months.

INTRODUCTION

There has been mounting evidence of the importance of aerosols in global climate change through their direct and indirect effects (IPCC, 2007). The magnitude of these effects is poorly constrained because of our limited knowledge of the processes that control the distributions as well as physical, chemical and optical properties of aerosols. Atmospheric aerosols and precursor gases exhibit large temporal and spatial variations due to variety of production, transport and removal processes. Aerosols in the boundary layer are directly produced from the natural and anthropogenic processes while those in the troposphere and aloft are largely due to gas-to-particle conversion processes. Hence, vertical (altitude-resolved) distributions of columnar aerosol and pre-cursor gas parameters in the height region, encompassing boundary- layer and free troposphere, play an important role in the transport and transformation of these constituents from source regions due to processes such as entrainment, mixing etc. Moreover, such measurements yield light extinction for a certain layer. Airborne measurements in this direction utilizing tracking sun-photometers (AATS) and coincident satellites (MODIS, TOMS, GOES) have been reported in the literature (Russell *et al.*, 1999; Livingston *et al.*, 2003, Shinozuka *et al.*, 2011). Combined lidar and sun-photometric measurements of columnar aerosol optical parameters over Taipei, Taiwan have been reported by Chen *et al.* (2009). Their results showed sensitivity of columnar water vapor on the association between aerosol extinction, size distribution and phase. Similar kind of measurements made over a tropical urban station (Pune, India) revealed that the trends in columnar AOD are not confined to boundary-layer but also extend up to stratospheric altitudes. In addition, the results indicated that the boundary-layer AOD contributes more than 20 per cent to the total column AOD (Devara *et al.*, 2012).

Measurements over high-altitude stations yield background levels of aerosol concentration (Arya and Jain, 1997; Reiter *et al.*, 1984; Mahadevan *et al.*, 1989; Jain, 2001; Dani *et al.*, 2003; Jain and Arya, 2004; Sagar *et al.*, 2004; Ghude *et al.*, 2005; Jain *et al.*, 2007; Gautam *et al.*, 2011; Srivastava *et al.*, 2012). So, it would be possible to examine and assess the extent to which the 'clean' remote areas have been affected by growing urbanization/industrialization (Jaenicke, 1979). Moreover, background sites with presumably cleaner environments and clear-sky conditions offer an excellent

* Corresponding author.
Tel.: +91-20-25904251; Fax: +91-20-25865142
E-mail address: devara@tropmet.res.in

opportunity to calibrate the performance of the optical monitoring sensors/equipment (Jayaraman, 1999; Sumit *et al.*, 2012). Added, these stations lie in the boundary-layer during daytime and in the free troposphere during the nighttime, thus provide good opportunity to investigate the transport/mixing of aerosols and gases from/between the boundary-layer to/and the free troposphere. Under seasonally varying wind patterns, these stations being in the free troposphere during night, becomes very important for regional study of transport of pollutants, particularly during early morning/night transition period.

Due to large heterogeneity in geography, climate, urbanization and population, the Indian subcontinent provides an interesting scenario where regional scale features would dominate distribution of any atmospheric constituent including aerosols. Systematic studies on atmospheric aerosols were initiated in India under the Indian Middle Atmosphere Program (IMAP) and Aerosol Climatology and Effects (ACE) projects (Krishnamoorthy *et al.*, 1999) of Indian Space Research Organization - Geosphere Biosphere Program (ISRO-GBP). Although, aerosol properties have been measured at many sites in India using direct and remote sensing techniques from ground, aircraft and ship in several campaign modes in the last more than two decades, only a few of them have fairly long-term data (Krishnamoorthy *et al.*, 1999; Devara *et al.*, 2002; Gautam *et al.*, 2009; Dey and Girolamo, 2010; Dani *et al.*, 2012 and others). In spite of unique importance, as explained above, aerosol measurements over high-altitude stations are very sparse (for example, hilly and forest regions in particular) in India (for example, Guleria *et al.*, 2012; Srivastava *et al.*, 2012; Vijayakumar and Devara, 2013). The present paper aims at (i) to obtain vertical distributions of aerosols and pre-cursor gases (ozone and precipitable water content in the present study) using a mobile dual multi-filter solar radiometer, (ii) to describe the experiments conducted at Sinhgad, a high-altitude, hill-top, remote (rural) station, and (iii) to present principle of operation of radiometers, method of data acquisition and analysis, and discuss the results obtained and summarize.

ABOUT EXPERIMENTAL SITE

The experimental station, Sinhgad (18°21′N, 73°43′E) is a rural (remote) hill station, about 40 km south-west of the city of Pune, India. It is situated on a hill rising 1450 m above mean sea level (AMSL). This fort is a twelfth century old structure and is one of the historical places in Maharashtra State. Fig. 1 illustrates the geographical location of Sinhgad and the associated enlarged picture below shows the view of a mountain-top area with experimental site (closed circle shown by an arrow), where the observations were carried out is a flat terrain with an area of about 0.5 square kilometers, and surface is composed of rocks and rock-dust. Other mountain peaks of comparable height also located in its neighborhood. This place is favored outing site for people in and around Pune during weekends. A few people live at the summit and some tourists visit the area (by foot). Human activities are generally more during the day time (1000–1800 hrs) whereas during night, very few people stay at the fort. As this site is situated in the complex of a Micro-wave tower building owned by Bharat Sanchar Nigam Limited (BSNL), Government of India, it is a protected area and trespassers or tourists are not allowed

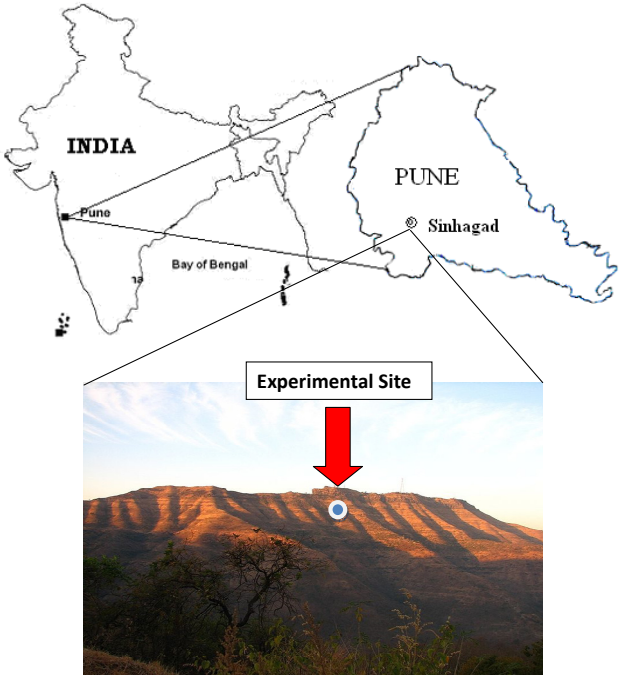

Fig. 1. India map depicting the Maharashtra State and locations of Pune and Sinhgad. Enlarged version of experimental site (hilltop) with an arrow showing the location (filled circle) where the radiometric observations were carried out is shown in a diagram beneath the map.

to enter. The only local source of pollution is wood-burning mainly for cooking and an intermittent small-scale vehicular traffic during daytime. In winter, the villagers burn the dry grass along the slope of the hill to make the way for their transit. Hence, the anabatic (warm upslope) flow during daytime and katabatic (cold down-slope) flow during nighttime are prevalent over the site. These flows help in formation and dissipation of haze within/from the valley floor during winter. During winter through pre-monsoon, the surrounding area is generally dry and production of major pollutants is from local sources such as domestic cooking and also some grass-burning or charcoal-making. Due to these typical conditions and far distance from urban activity, Sinhgad is considered as a rural background location. The weather at Sinhgad during November to February months comprises a synoptic northwesterly to northeasterly circulation, dry ambient atmosphere with relative humidity ~30 to 70% and scanty rainfall. The temperature varies from 4°C (nighttime) to 35°C (daytime). The December month is the coolest of all months with lowest occurring nighttime temperature. The winds are highly variable during daytime. The experimental station experiences aerosol pollution in the boundary-layer during winter season due to its valley-like configuration and associated meteorology.

SOLAR RADIOMETER, PRINCIPLE OF OPERATION, DATA ARCHIVAL AND METHOD OF ANALYSIS

Two compact, on-line, multi-filter solar radiometers (MICROTOPS-II, Sunphotometer Model 540 and Ozonometer Model 521, manufactured by M/s Solar Light Co., USA, factory-calibrated every year) were used in the present study. Fig. 2 displays photograph of the multi-filter solar radiometer of both sun-photometer and ozone versions, mounted on a wooden platform fixed to a tripod for achieving high stability, time synchronization between observations and easy focusing of radiometer to the Sun's disk. Each channel is fitted with a narrow-band filter and a Gallium Phosphide detector. The radiation, captured by the collimator and band-passed by the filters falls onto the photodiode, produces an electrical output proportional to radiant power (irradiance). These outputs measured at each filter are amplified and analog-to-digital converted, and finally stored, together with the time of observation provided by the built-in master clock, in the memory for further analysis. The radiometer is equipped with built-in algorithms for computing ozone, precipitable water content and AOD from the output of the amplifier recorded for each filter. Dual multi-filter solar radiometers equipped with Global Positioning System (GPS) and automatic weather monitor, carried with a vehicle, have been used for the measurement of aerosols, ozone, precipitable water content along with met parameters (pressure, temperature and wind).

Observations were carried out from bottom of the hill to top/peak, thus at different altitudes during the mobile track having atmospheric pressure difference of about 75 mb, covering over 12 height intervals. Each set of observations, covering all these pressure (altitude) levels, took less than an hour. On some experimental days, measurements were made both during onward and return journey. For each measurement, the site location (latitude and longitude) and pressure values have been fed to the sun-photometer/ ozonometer as per the instrument's requirement. The instruments were operated concurrently and obtained instantaneous values of AOD, TCO, PWC and meteorological parameters at each altitude on clear-sky days. The vehicle's engine was put off during the measurements to avoid contamination due to vehicular emissions. The variations in solar irradiance measured for different solar zenith angles (air mass) at each filter have been used for obtaining aerosol optical depth (AOD). The variations in AOD for spectral bands centered at 380, 440, 500, 675, 870 and 1020 nm have been utilized to retrieve columnar aerosol size distribution (ASD). The TCO and PWC were obtained by following the differential optical absorption method, applied to the irradiance observed by the radiometer around the UV and NIR wavelengths. A brief description of the methodology is given below.

Solar radiation traversing through the terrestrial atmosphere undergoes extinction due to three processes, namely, Rayleigh scattering by air molecules, Mie scattering by aerosols, and molecular absorption. Solar radiation is a composite of monochromatic radiations. Molecular and ozone (significant

Fig. 2. Photograph showing portable multi-filter dual radiometer.

absorbing gas in the wavelength band considered in the present study) optical depths were computed by using the expression of Kneizys *et al.* (1980) and Teillet (1990), respectively. The sun photometer works on the principle of measuring the solar radiation intensity at some specified wavelengths and converts it to optical depth by knowing the corresponding intensities at the top of the atmosphere (TOA). The TOA irradiance at each wavelength was calculated via the well-known Langley method. For this, the expression given by Kasten and Young (1989) for the air mass computation was used. The instrument measures the irradiance signals at different wavelengths in mV, from which the absolute irradiance in Wm^{-2} is obtained by multiplying the signal with calibration factor (Wm^{-2}/mV). The calibration relies on a high-performance voltage reference with the temperature coefficient ≤ 0.001% per degree Celsius and long-term stability of ~0.005% per year. As suggested by Devara *et al.* (2001), Morys *et al.* (2001), Porter *et al.* (2001) and many others, determination of zero air mass intercept is one of the important sensitive parameters in the retrieval of AOD, TCO and PWC from sun photometric measurements. Typically, a 0.5% error in the zero air mass measurement gives 0.005 error in optical depth at low air mass. Moreover, the zeros air mass value serves as calibration constant when it is corrected for mean sun-earth distance (typically above 60° solar zenith angle). Possible error sources in the determination of this parameter and solutions have been discussed in the literature (Shaw, 1976; Kremser *et al.*, 1984; Kasten and Young, 1989; Devara *et al.*, 1996). At larger air mass, the errors in AOD decrease. This is the reason why most of the satellites, which are used to derive AOD make measurements near noon solar time. The full width at half maximum bandwidth at each of these wavelength channels is 2.4 ± 0.4 nm, and the accuracy of the sun-targeting angle is better than 0.1°.

Having obtained AOD at different wavelengths, aerosol size distribution (ASD) has been retrieved from the spectral variation of AOD by following the constrained linear inversion scheme (King *et al.*, 1978; King, 1982) with the Fredholm integral as

$$\tau_a(\lambda) = \int_0^\infty \Pi r^2 Q_{ext}(r,\lambda,m)\, n_c(r) dr \quad (1)$$

where r is the particle radius, m is the complex refractive index of aerosol particles, $Q_{ext}(r,\lambda,m)$ is the Mie extinction efficiency parameter and $n_c(r)$ is the columnar size distribution. Since $n_c(r)$ cannot be written analytically, a numerical approach is followed to separate $n_c(r)$ into two parts as $n_c(r) = h(r)\cdot f(r)$, where h(r) is rapidly varying function with r and f(r) is slowly varying. Hence the above equation changes to

$$\tau_a(\lambda) = \sum_{j=1}^{q} \int_{r_j}^{r_j=1} \Pi r^2 Q_{ext}(r,\lambda,m)\, h(r)\, f(r) dr \quad (2)$$

In Eq. (2), the quadrature error will be less if f(r) is assumed to be constant. In that case, a system of linear equations results, which may be written as

$$\tau_a(\lambda) = A\, f(r) + \varepsilon \quad (3)$$

where $A = \int \Pi r^2 Q_{ext}(r,\lambda,m)\, h(r) dr$ and ε is an error which arises due to deviation between the measured τ_a and theoretical τ_a ($= \sum A_{ij}.f_i$). Initially, the Junge exponent (ν) is computed from the wavelength dependence of AOD and used as a zero-order weighting function, $h_0(r)$. By using $h_0(r)$ as an initial guess, first order $f^{(1)}$ values are evaluated using the equation

$$f^{(1)} = (A^T S_\varepsilon^{-1} A + \gamma H)^{-1} A^T S_\varepsilon^{-1} \tau_a \quad (4)$$

where γ is non-negative Lagrangian multiplier and S_ε is the measured covariance matrix, H is a mean diagonal matrix and superscript T denotes matrix transposition. This iteration procedure is repeated until the observed τ_a comes closer to the re-computed τ_a.

The total column ozone (TCO, expressed in DU), which is equivalent to thickness of pure ozone layer at standard temperature and pressure, is measured by recording differential absorption of solar light intensity at wavelengths in the UV region (305.5 nm and 320 nm). The measurement at the third wavelength (312.5 nm) is used to correct for particulate scattering and stray light. The columnar precipitable water content (PWC, expressed in cm) is obtained from the radiance measurements made at 940 nm and 1020 nm channels of the radiometer. The estimation of PWC was made by following the differential optical absorption method applied the irradiance data archived at 940 nm (maximum absorption for water vapor) and at 1020 nm (less absorption or almost transmission for water vapor). More description of the instrument and method of deriving AOD, TCO and PWC from the solar irradiance observations including mathematical formulations can be found in the literature (Devara *et al.*, 2001, 2005). Albeit the experiments were conducted on many days, useful observations could be obtained only on a limited number of days due to unfavorable sky conditions. Thus the archived clear-sky data on column-integrated aerosols, ozone and precipitable water content on three typical winter days, namely, 16 December 2002, 03 and 21 January 2003 are presented and discussed in the following sections. Experiment was conducted only during ascent (onward journey) on 16 December 2002 whereas observations were obtained both during ascent (onward) and descent (return journey) on 03 and 21 January 2003.

RESULTS AND DISCUSSION

From the instantaneous solar flux measurements, columnar AODs at six wavelengths, each centered at 380, 440, 500, 675, 870 and 1020 nm have been evaluated using the internal calibration involving (i) internal barometer/altimeter for monitoring of atmospheric pressure and altitude of the experimental location, and (ii) global positioning system (GPS) receiver that provides the geographical coordinates of the location used for estimating the local air mass. The

ozone monitor used in the present experiment utilizes the solar irradiance measured at three UV wavelengths, each centered at 305.5, 320 and 312.5 nm. The columnar PWC was obtained from the radiance measured at two NIR wavelengths centered at 940 and 1020 nm. Thus the measured AODs at the wavelengths of 380, 440, 500, 675, 870 and 1020 nm were utilized to retrieve columnar aerosol size distribution by applying the constrained liner inversion method developed by King *et al.* (1978). Meteorological parameters greatly influence the aerosol properties (Hänel, 1976; Nilsson, 1979; Devara *et al.*, 1994). Temperature and relative humidity variations lead to gas-to-particle conversion and higher wind speeds which may result in horizontal advection of pollution leading to higher AOD and modified ASD.

Vertical Distributions

Features Observed on 16 December 2002

The height profiles of AOD, TCO and PWC along with meteorological parameters (wind, dry-bulb and wet-bulb temperatures) observed on 16 December 2002 are shown plotted in Figs. 3(a)–3(c). It is evident from the figure that AOD at all the three characteristic wavelengths decreases with increase in altitude. Moreover, the wavelength dependency (lower AOD at longer wavelength) in these variations can also be seen, particularly in the lower altitudes, which is consistent with the Mie theory. The coarse-mode particles (AODs at 1020 nm) are found to deviate from those at 380 nm and 500 nm, indicating different aerosol chemical and growth processes. The ozone profile started with low value initially, increased to 260 DU around 925 mb and thereafter maintained constant except a layer formation at around 900 mb level, showing almost similar structure as that of AOD. Like AOD, PWC also showed decrease with increase in altitude with a structure around 900 mb. Furthermore, all the three profiles of AOD, PWC and TCO exhibit significant layer structures, similar to those seen in the concurrent wind and temperature profiles. This reveals that the local meteorological parameters play significant role in the altitude structures of AOD, PWC and TCO.

Fig. 4 displays variation of columnar aerosol size distribution (ASD) on 16 December 2002, inverted from the spectral distribution of AOD at different pressure levels (altitudes), following the constrained linear numerical inversion scheme as suggested by King *et al.* (1978) and King (1982). Each frame of the figure shows a plot of dNc/dlogR, representing the number of particles per unit area per unit log radius interval in a vertical column through the atmosphere versus the radius in microns. Significant changes in ASD due to sudden changes in wind and temperature (both dry-bulb and wet-bulb) can be noted during the study period. One common feature that can be seen in all the size spectra is the dominance of fine-mode particles. Mostly mono- and at some altitudes, bi-modal distributions are seen on this day. This implies that both natural and anthropogenic sources are prevailing over the experimental site, with predominant accumulation-mode particles at higher altitudes resulting from long-range transport phenomenon.

Features Observed on 03 January 2003

On 03 January 2003, the experiment was conducted while ascending to and descending from the experimental site. The vertical profiles of AOD, TCO and PWC together with concurrent meteorological parameters during both onward and return journeys are depicted in Figs. 5(a)–5(f). Compared to 16 December 2002, the values of AOD, PWC and TCO are higher on 03 January 2003, which may be due to time of observation. This can also be seen from the dry-bulb temperature recorded on both days. The experiment commenced around 0700 hrs on 16 December 2002 while it started around 1000 hrs on 03 January 2003. So, the aerosol emissions were low on 16 December as compared to 03 January. It can be seen from the figure that there are no much variations in height distribution of multi-spectral AODs, but the wavelength dependency can well be seen. Even though the variations are smaller, two aerosol layers, one around 920 mb and another around 880 mb levels can be seen, which are considered to be due to local meteorology, particularly driven by the wind field. The TCO variations appear to be smaller around a mean value of 290 DU while

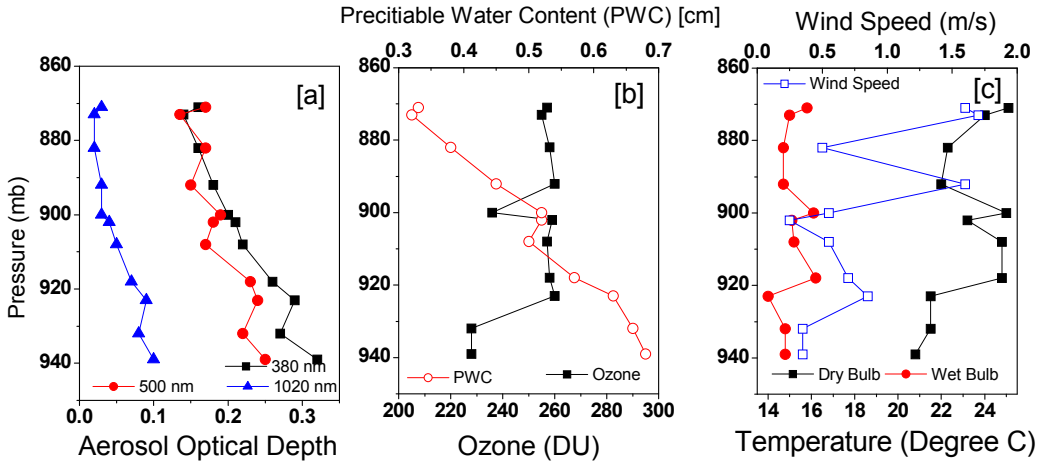

Fig. 3. Radiometer-derived altitudinal (pressure) distribution of aerosol optical depth [a], water vapor and ozone [b] and meteorological parameters [c] on 16 December 2002.

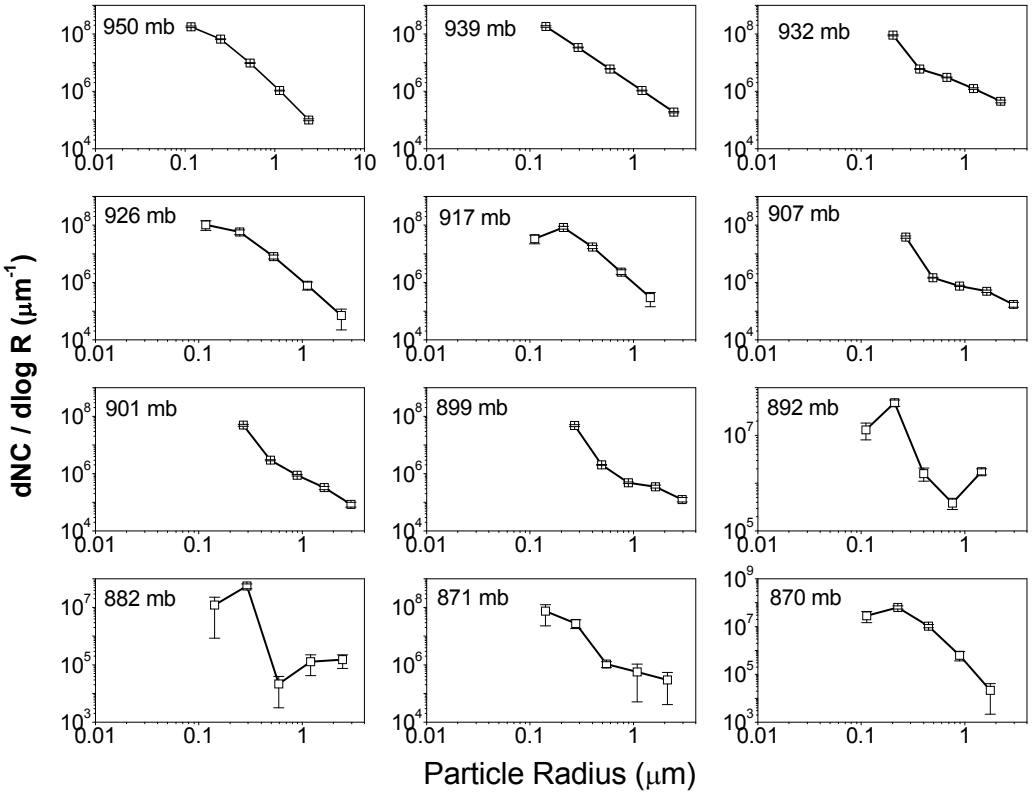

Fig. 4. Aerosol size distribution at different pressure levels observed on 16 December 2002.

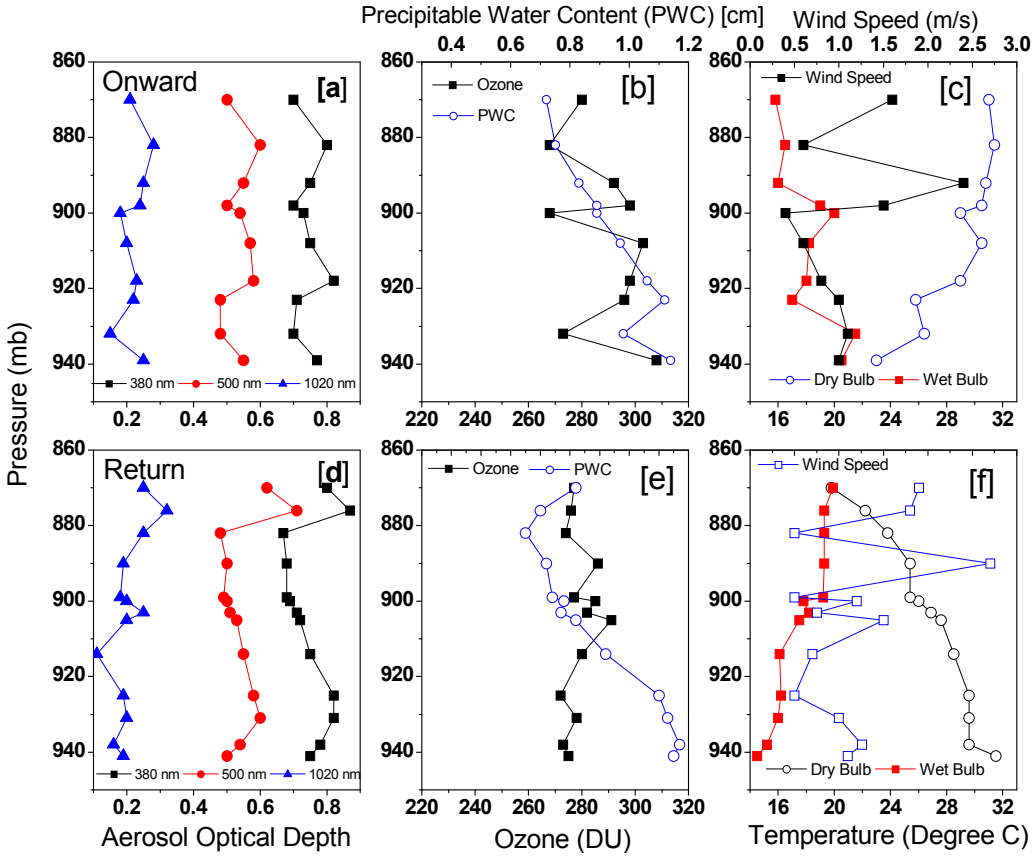

Fig. 5. Altitudinal variation of AOD [a], ozone and water vapor [b] and meteorological parameters [c] during onward journey and the same parameters during return journey [d, e, f] observed on 03 January 2003.

the PWC decreased with increase in altitude. The variations in AOD, TCO and PWC during return journey (descending) are seen to be similar to those during the onward journey (ascending) except at the initial portion of the AOD profiles. The initial decreasing trend during ascending and increasing trend during descending are considered to be due to difference in aerosol emissions at the lower levels. This can be understood from the dry-bulb temperature profiles recorded during both journeys. The aerosol layer formations and the responsible concurrent meteorological parameters seem to be similar for both journeys.

The height variation of aerosol size spectra during onward and return journeys are shown in Figs. 6 and 7, respectively. During both phases, the size spectra at all altitudes appear to follow power-law distribution except at 937 mb level where the spectrum shows mono-modal distribution. However, all the spectra show predominant fine-mode aerosol particles originating from domestic cooking or waste-burning activities associated with convective activity which lifts the fine-mode particles up (thereby dilution in the lower and accumulation in the upper altitudes) in the experimental region, as compared to the earlier experiment conducted in the December month. Thus a sparse contribution from wind-driven fine soil-dust cannot be ruled out.

Features Observed on 21 January 2003

Figs. 8(a)–8(c) depicts the height variation of multi-wavelength AOD, PWC and TCO during both onward and return journeys on 21 January 2003. It was not possible to record meteorological parameters due to some technical problems. Except TCO, AOD and PWC showed decrease with increase in altitude. In contrast, the AOD profiles showed some fluctuations around respective mean values. Interestingly, all the profiles show a prominent peak around 920 mb pressure level which is considered to be due to sudden wind gradient around that altitude. Aerosol size distributions during onward and return journeys on 21 January 2003 are shown in Figs. 9 and 10, respectively. The size spectra on this day during ascent are found to be different from those during the descent period. The ascent spectra showed mostly bi-modal distribution involving both fine and coarse-mode aerosol particles from natural and anthropogenic sources, and at times the spectra showed power-law distribution with different slopes. The spectra during return journey show power-law or mono-modal distribution almost at all altitudes considered in the study. This implies that the relative contrast in convective activity between the onward and return journeys contributed more number of fine aerosol particles ejected from the lower parts of the atmosphere to higher altitudes.

Comparison with Other Sites

The heterogeneity in space-time variations in aerosol distributions mainly comes from the geographical location and/or experimental terrain, which modifies the wind flow patterns, of the experimental site. In this context, aerosol or pre-cursor gas concentrations over high-altitude sites (in the absence of local pollution sources and long-range transport)

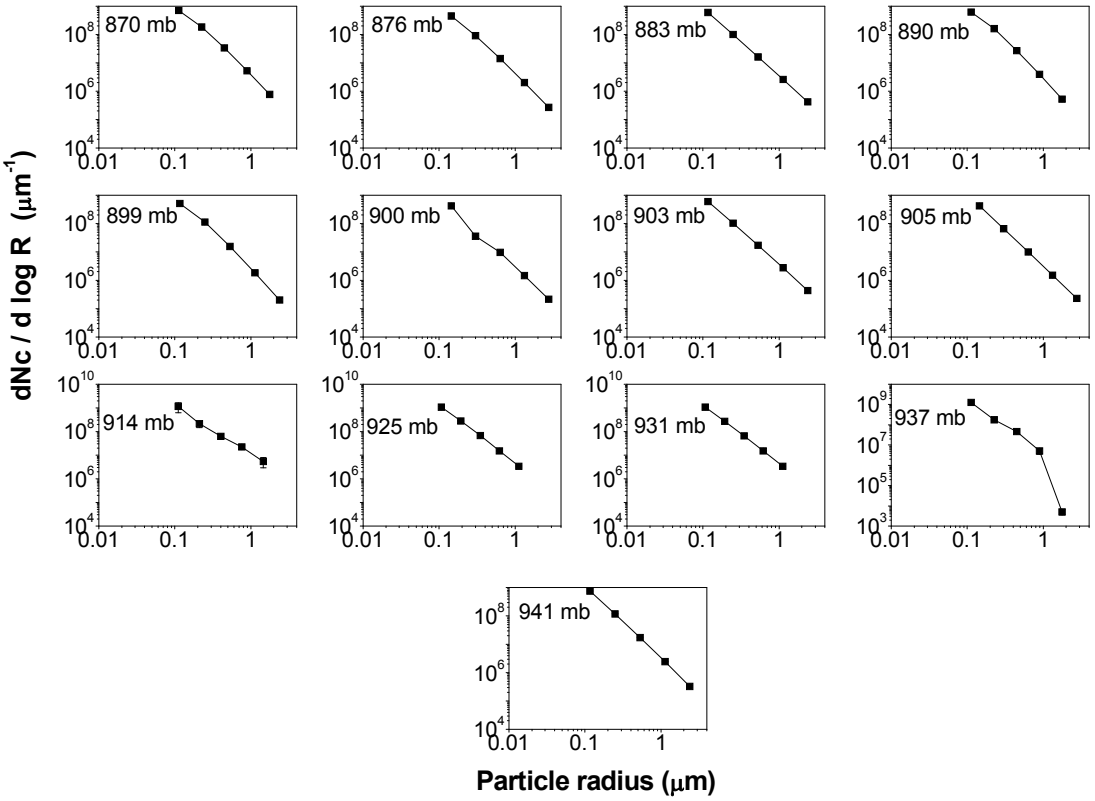

Fig. 6. Radiometer-derived aerosol size distributions at different pressure levels during onward journey on 03 January 2003.

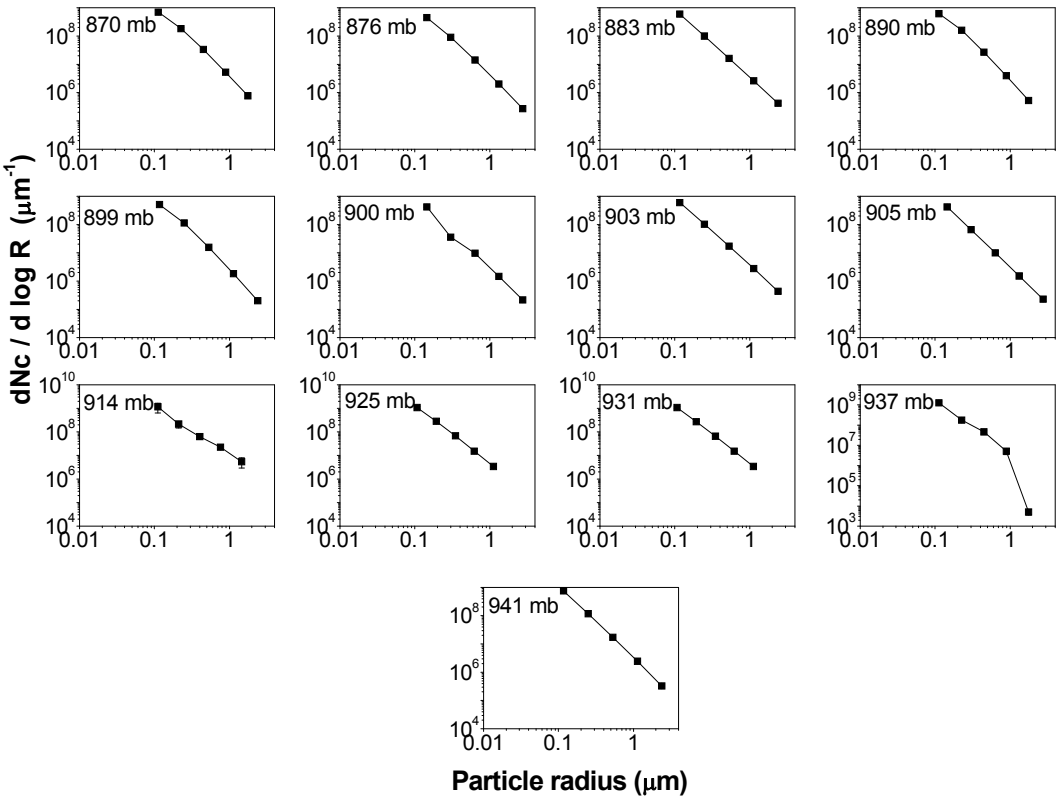

Fig. 7. Same as Fig. 6 but during return journey.

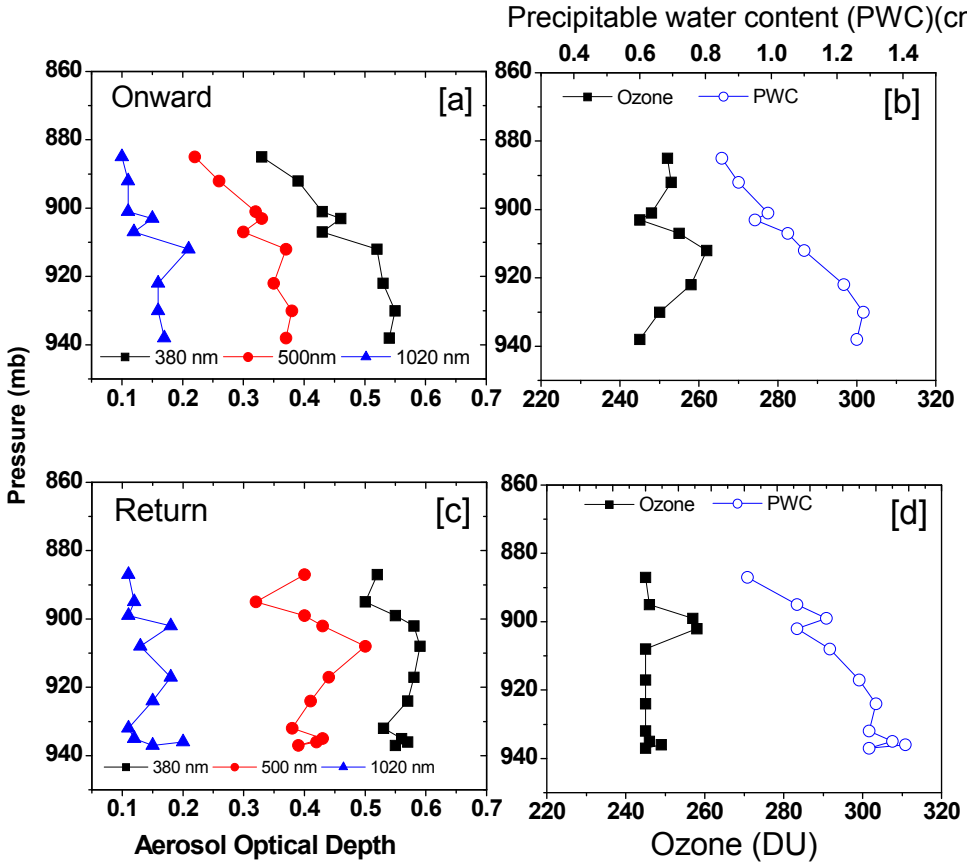

Fig. 8. Height variation of AOD [a] and TCO and PWC [b] during onward journey and the same during return journey [c, d] on 21 January 2003.

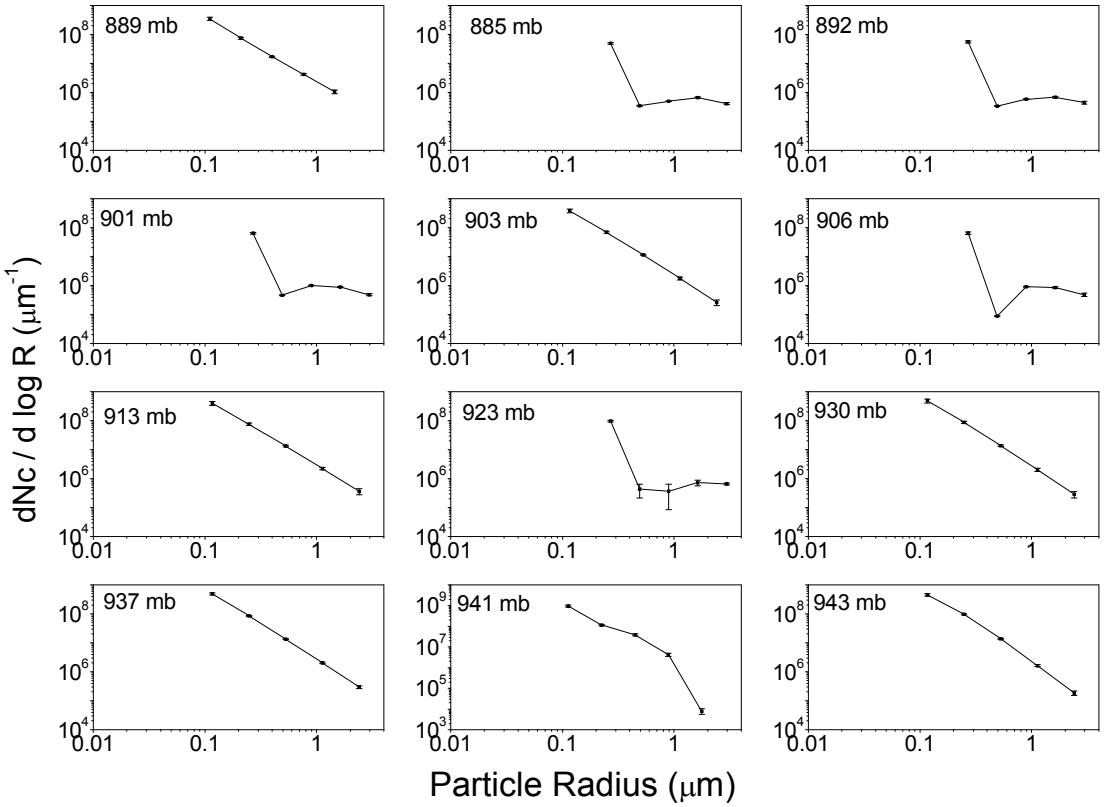

Fig. 9. Height variation of aerosol size distribution during onward journey on 21 January 2003.

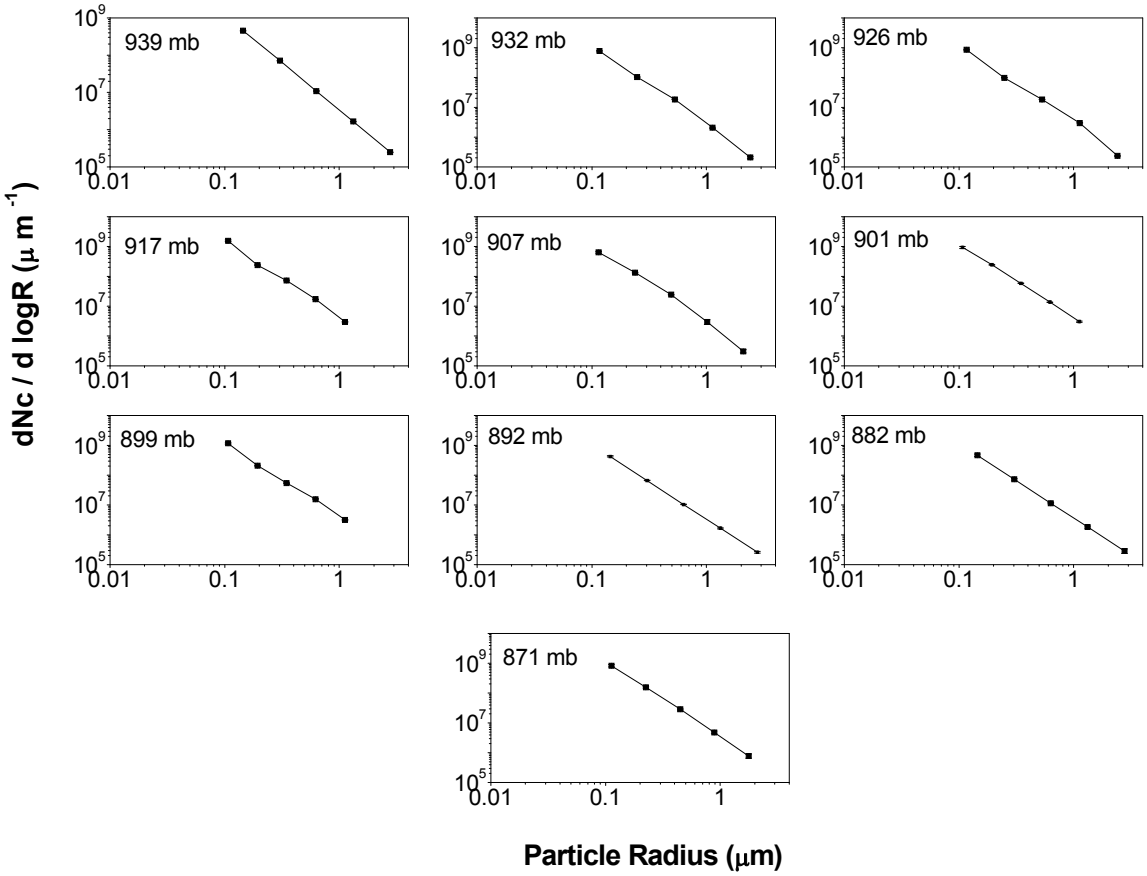

Fig. 10. Same as Fig. 9 but during return journey.

represent background levels, against which the aerosol trends at any site can be evaluated. The complex terrains often complicate the situation. Albeit many high-altitude stations are established over the world, due to unknown degree of variability in natural versus anthropogenic source concentrations, these stations should be used with caution for estimating reliable trends. The columnar AOD, PWC and TCO measured by using ground-based solar radiometer from the present study are compared with those measured at other high-altitude stations of Northern India (Dani *et al.*, 2003; Jain and Arya, 2004; Sagar *et al.*, 2004), and a near-by urban station (Pune) of Central India in Table 1. Two major points are clear from the table – (i) aerosol and pre-cursor gases at remote high altitude locations were different from those observed at highly polluted urban locations, inverse relationship between AOD and station altitude and (ii) short-term changes in AOD, PWC and TCO can be attributed mainly due to changes in the properties and loading of aerosols in the atmospheric boundary-layer over the observing stations. It may be noted here that time-synchronized multi-site measurements (considering elevation of each site as altitude) in a close proximity can also provide height profiles of atmospheric constituents, but in the present study, such profiles at single station by making measurements during the ascent and descent have been demonstrated with better space-time resolution.

SUMMARY AND CONCLUSION

A novel approach wherein portable, on-line, multi-filter, solar radiometers have been used to investigate the vertical distributions of columnar AOD, TCO and PWC over Sinhgad, a high-altitude, rural station. The results obtained on three typical experimental days during the winter of 2002–2003 are presented. The wavelength dependence of AOD is found in accordance with the Mie theory. The aerosol size distributions, inverted from the spectral distribution of AOD revealed, height variation of aerosol size spectra involving mono- and bi-modal distributions, mixing of the local and long-range transported aerosols. The space-time variations in AOD, TCO and PWC and the associated layer structures are noticed to be with local meteorological conditions. The

Table 1. Comparison of AOD, TCO and PWC between rural (high-altitude) and urban stations.

Station[#]	Aerosol Optical Depth at wavelength of						Ozone (DU)	Precipitable Water Content (cm)
	380 nm	440 nm	500 nm	675 nm	870 nm	1020 nm		
Mohal 20-31 May 2000	0.6	0.58	0.47	0.35	0.33	0.31	275.60	1.460
Kothi 20-31May 2000	0.35	0.37	0.28	0.22	0.23	0.26	258.1	0.451
Rahala Falls 20-31May 2000	0.27	0.28	0.19	0.14	0.18	0.22	260.9	0.320
Madhi 20-31May 2000	0.21	0.24	0.14	0.10	0.15	0.19	260.4	0.114
Rothang Pass 20-31May 2000	0.20	0.23	0.12	0.08	0.14	0.23	251.5	0.044
Sinhgad 16 December 2002	0.24	0.28	0.18	0.13	0.12	0.07	261.00	0.455
Pune 17 December 2002	0.44	0.44	0.36	0.27	0.21	0.17	250.60	0.683
Sinhgad 3 January 2003	0.75	0.67	0.57	0.38	0.30	0.24	278.60	0.778
Pune 2 January 2003	0.70	0.60	0.50	0.33	0.31	0.24	268.27	0.780
Sinhgad 21 January 2003	0.40	0.38	0.29	0.20	0.18	0.16	250.34	0.857
Pune 23 January 2003	0.37	0.34	0.26	0.18	0.11	0.15	254.23	0.790
Nainital December 2002	-	-	0.12	-	-	-	-	1.260
Leh July 2003	-	-	-	-	-	0.09	281.60	0.749
Hanle July 2003	-	-	-	-	-	0.03	276.00	0.420

[#] Pune (18°32′N, 73°51′E, 559 m AMSL); Mohal (31°54′N, 77°07′E, 1100 m AMSL); Sinhgad (18°21′N, 73°43′E, 1313 m AMSL); Kothi (32°54′N, 77°11′E, 2821 m AMSL); Rahala Falls (32°20′N, 77°12′E, 3078 m AMSL); Madhi (32°21′N, 77°13′E, 3278 m AMSL); Rothang Pass (32°22′N, 28°37′N, 4112 m AMSL); Nainital (29°22′N, 79°27′E, 2200 m); Leh (34°15′N, 77°36′E, 3311 m AMSL); Hanle (32°47′N, 78°58′E, 4500 AMSL).

experimental approach presented here would be useful to obtain vertical profiles of AOD, TCO and PWC using portable radiometers carried by vehicle over hilly/mountain regions. Such an approach yields profiles of AOD and pre-cursor gases over areas with scarce alternative measurements, networks with sporadic presence of ground sites and limited number of satellite retrievals. It is being planned to re-visit the site by repeating similar experiments during different seasons over a longer period to understand the influence of latest developments in the form of land-use pattern changes and associated anthropogenic activities such as road construction, irrigation, and plantation etc. on regional climate.

ACKNOWLEDGEMENTS

The hand-held meteorological kit for this study was provided by the India Meteorological Department (IMD), Pune. The authors are also thankful to the authorities of BSNL, Pune at Sinhgad site and the Director, IITM for necessary support. The insightful comments and useful suggestions of Prof. Moo-Been Chang, the Editor of the journal and the two anonymous reviewers are gratefully acknowledged.

REFERENCES

Arya, B.C. and Jain, S.L. (1997). Measurement of Water Vapor at Maitri, Antarctica. *Indian J. Radio Space Phys.* 26: 117–120.

Chatterjee, A., Ghosh, S.K., Adak, A., Devara, P.C.S. and Raha, S. (2012). Effect of Dust and Anthropogenic Aerosols on Columnar Aerosol Optical Properties over Darjeeling (2200 m asl), Eastern Himalayas, India. *PLoS ONE* 7: 1–10.

Chen, W.N., Chen, Y.W., Chou, C.C.K., Chang, S.Y., Lin, P.H. and Chen, J.P. (2009). Columnar Optical Properties of Tropospheric Aerosol by Combined Lidar and Sunphotometer Measurements at Taipei, Taiwan. *Atmos. Environ.* 43: 2700–2708.

Dani, K.K., Raj, P.E., Maheskumar, R.S. and Devara, P.C.S. (2003). Measurement of Columnar Aerosol, Ozone and Precipitable Water at Some High Altitude Sites in North India. *Indian J. Environ. Prot.* 23: 126–138.

Dani, K.K., Raj, P.E., Devara, P.C.S., Pandithurai, G., Sonbawne, S.M., Maheskumar, R.S., Saha, S.K. and Jaya Rao, Y. (2010). Long-term Trends and Variability in Measured Multi-spectral Aerosol Optical Depth over a Tropical Urban Station in India. *Int. J. Climatol.* 32: 153–160.

Devara, P.C.S., Raj, P.E., Sharma, S. and Pandithurai, G. (1994). Lidar Observed Long-term Variations in Urban Aerosol Characteristics and Their Connection with Meteorological Parameters. *Int. J. Climatol.* 14: 581–591.

Devara, P.C.S., Pandithurai, G., Raj, P.E. and Sharma, S. (1996). Investigations of Aerosol Optical Depth Variations Using Spectroradiometer at an Urban Station, Pune, India. *J. Aerosol Sci.* 27: 621–632.

Devara, P.C.S., Maheskumar, R.S., Raj, P.E., Dani, K.K. and Sonbawne, S.M. (2001). Some Features of Columnar Aerosol Optical Depth, Ozone and Precipitable Water Content Observed over Land during the INDOEX-IFP99. *Meteorol. Z.* 10: 123–130.

Devara, P.C.S., Maheskumar, R.S., Raj, P.E., Pandithurai, G. and Dani, K.K. (2002). Recent Trends in Aerosol Climatology and Air Pollution as Inferred from Multi-year Lidar Observations over A Tropical Urban station. *Int. J. Climatol.* 22: 435–449.

Devara, P.C.S., Saha, S.K., Raj, P.E., Sonbawne, S.M., Dani, K.K., Tiwari, Y.K. and Maheskumar, R.S. (2005). A Four-year Climatology of Total Column Tropical Urban Aerosol, Ozone and Water Vapor Distributions over Pune, India. *Aerosol Air Qual. Res.* 5: 103–114.

Dey, S. and Di Girolamo, L. (2010). A Climatology of Aerosol Optical and Microphysical Properties over the Indian Sub-continent from 9 Years (2000-2008) of Multi-angle Imaging Spectroradiometer (MISR) Data. *J. Geophys. Res.* 115: D15204.

Gautam, R., Hsu, N.C., Lau, K.M., Tsay, S.C. and Kafatos, M. (2009). Enhanced Pre-monsoon Warming over the Himalayan-Gangetic Region from 1979 to 2007. *Geophys. Res. Lett.* 36: L07704, doi: 10.1029/2009GL037641.

Gautam, R., Hsu, N.C., Tsay, S.C., Lau, K.M., Holben, B.N., Bell, S., Smirnov, A., Li, C., Hansell, R., Ji, Q., Payra, S., Arya, D., Kayastha, R. and Kim, K.M. (2011). Accumulation of Aerosols over the Indo-Gangetic Plains and Southern Slopes of the Himalayas: Distribution, Properties and Radiative Effects during the 2009 Pre-monsoon Season. *Atmos. Chem. Phys.* 11: 12841–12863.

Ghude, S.D., Jain, S.L., Arya, B.C. and Bajaj, M.M. (2005). Comparison of Total Column Water Vapor Measured at New Delhi, Leh, Hanle and Maitri (Antarctica). *Indian J. Radio Space Phys.* 34: 264–268.

Guleria, R.P., Kuniyal, J.C., Rawat, P.S., Sharma, N.L., Thakur, H.K., Dhyani, P.P. and Singh, M. (2012). The Assessment of Aerosol Optical Properties over Mohal in the Northwestern India Himalayas Using Satellite and Ground-based Measurements and an Influence of Aerosol Transport on Aerosol Radiative Forcing. *Meteorol. Atmos. Phys.* 113: 153–169.

Hänel, G. (1976). The Properties of Atmospheric Aerosol Particles as Function of Relative Humidity at Thermodynamic Equilibrium with Surrounding Moist Air. *Adv. Geophys.* 19: 73–188.

IPCC (2007). Summary for Policymakers, In *Climate Change 2007*: *The Physical Science Basis*, Intergovernmental Panel on Climate Change, Solomon, S., Qin, D., Manning, M., Enhen, Z., Marquis, M., Averyt, K.B., Tignor, M. and Miller, H.L. (Eds.), Cambridge University Press, Cambridge, United Kingdom and New York, USA, 1056 pp.

Jaenicke, R. (1979). Measurements of Aitken Nuclei in Extremely Clean Air in Tasmania. *J. Aerosol Sci.* 10: 205–207.

Jain, S.L. (2001). Monitoring of Ozone, Water Vapor etc. during the Voyage to Antarctica. *Asian J. Phys.* 10: 315–321.

Jain, S.L. and Arya, B.C. (2004). Measurement of Solar Radiation at New Delhi, High Altitude Observatory,

Hanle and Maitri Antarctica. 35 COSPAR Scientific Assembly, 18-25 July 2004, Paris, France, p. 309.

Jain, S.L., Kulkarni, P.S., Arya, B.C., Kumar, A., Ghude, S.D. and Singh, P. (2007). Altitudinal Variation of Surface Aerosol with Change in Site: A Comparative Study. *Indian J. Radio Space Phys.* 36: 571–575.

Jayaraman, A. (1999). Results on Direct Radiative Forcing of Aerosol Obtained over the Tropical Indian Ocean. *Curr. Sci.* 67: 924–930.

Kasten, F. and Young, A.T. (1989). Revised Optical Air Mass Tables and Approximation Formula. *Appl. Opt.* 28: 4735–4738.

King, M.D., Byrne, D.M, Herman, B.M. and Reagan, J.A. (1978). Aerosol Size Distributions Obtained by Inversion of Spectral Optical Depth Measurements. *J. Atmos. Sci.* 35: 2153–2167.

King, M.D. (1982). Sensitivity of Constrained Linear Inversion to the Selection of Lagrange Multiplier. *J. Atmos. Sci.* 39: 1356–1369.

Kneizys, F.X., Shettle, E.P., Gallery, W.O., Chetwynd, J.H., Abreau, L.W., Selby, J.E.A., Fenn, R.W. and McClatchy, R.A. (1980). Atmospheric Transmittance/Radiance Computer Code LOWTRAN 5, AFGL-TR-80-00067, U.S. Air Force Environ res. Paper No. 697.

Kremser, H., Koepke, P. and Quenzel, H. (1984). Aerosol Optical Thickness from Direct Solar Radiation: Improved Langley Method Applied to Measured Data, IRS 1984: Current Problems in Atmospheric Radiation, Proc. Inst. Radiation Symposium, Fiocco, G. (Eds.), Deepak Publishing, New York.

Krishnamoorthy, K. (1999). Aerosol Climatology over India, ISRO-GBP Scientific Report, ISRO-GBP-SR-O3-99, 1-30.

Livingston, J.M., Russell, P.B., Reid, J.S., Redemann, J., Schmid, B., Allen, D.A., Torres, O., Levy, R.C., Remer, L.A., Holben, B.N., Smirnov, A., Dubovik, O., Welton, E.J., Campbell, J.R., Wang, J. and Christopher, S.A. (2003). Airborne Sun Photometer Measurements of Aerosol Optical Depth and Columnar Water Vapor during the Puerto Rico Dust Experiment and Comparison with Land, Aircraft, and Satellite Measurements. *J. Geophys. Res.* 108: 8588, doi: 10.1029/2002JD002520.

Mahadevan, T.N., Negi, B.S. and Meenakshy, V. (1989). Measurements of Elemental Composition of Aerosol Matter and Precipitation from a Remote Background Site in India. *Atmos. Environ.* 23: 869–874.

Morys, M., Mims III, F.M., Hangerup, S., Anderson, S.E., Baker, A., Kia, J. and Walkup, T. (2001). Design, Calibration, and Performance of MICROTOPS II Handheld Ozone Monitor and Sun photometer. *J. Geophys. Res.* 106: 14573–14582.

Nilsson, B. (1979). Meteorological Influence on Aerosol Extinction in the 0.2-40 μm Wavelength Range. *Appl. Opt.* 18: 3457–3473.

Reiter, R., Carnuth, W. and Sladkovic, R. (1984). Determination of Physical and Chemical Properties of the Aerosol from 1972 to 1982 at North Alpine Pure Air Station at 1780 m.a.s.l. *Arch. Meteorol. Geophys. Bioklimatol. A* B35: 179–201.

Russell, P.B., Livingston, J.M., Hingnett, P., Kinne, S., Wong, J. and Hobbs, P.V. (1999). Aerosol-induced Relative Flux Changes off the United States Mid-Atlantic Coast: Comparison of Values Calculated from Sun Photometer and In-situ Data with Those Measured by Airborne Pyranometer. *J. Geophys. Res.* 104: 2289–2307.

Sagar, R., Kumar, B., Dumka, U.C., Krishnamoorthy, K. and Pant, P. (2004). Characteristics of Aerosol Spectral Optical Depths over Manora Peak: A High-altitude Station in the Central Himalayas. *J. Geophys. Res.* 109: D06207, doi: 10.1029/2003JD003954.

Shaw, G.E. (1976). Error Analysis of Multi-wavelength Sunphotometry. *Pure Appl. Geophys.* 114: 1–4.

Shinozuka, Y., Redemann, J., Livingston, J.M., Russell, P.B., Clarke, A.D., Howell, S.G., Freitag, S., O'Neill, N.T., Reid, E.A., Johnson, R., Ramachandran, S., McNaughton, C.S., Kapustin, V.N., Brekhovskikh, V., Holben, B.N. and McArthur, L.J.B. (2011). Airborne Observation of Aerosol Optical Depth during ARCTAS: Vertical Profiles, Inter-Comparison and Fine-mode Fraction. *Atmos. Chem. Phys.* 11: 3673–3688.

Srivastava, A.K., Dey, S. and Tripathi, S.N. (2012). Aerosol Characteristics over the Indo-Gangetic Basin: Implications to Regional Climate, In *Atmospheric Aerosols-Regional Characteristics-Chemistry and Physics*. Chapter 3: 47–80.

Sumit, K., Devara, P.C.S. and Manoj, M.G. (2012). Multi-site Characterization of Tropical Aerosols: Implications for Regional Radiative Forcing. *Atmos. Res.* 106: 71–85.

Teillet, P.M. (2002). Rayleigh Optical Depth Comparison from Various Sources. *Appl. Opt.* 29: 1897–1900.

Vijayakumar, K. and Devara, P.C.S. (2013). Study of Aerosol Optical Depth, Ozone, and Precipitable Water Content over Sinhgad, a High-altitude Station in the Western Ghats. *Int. J. Remote Sens.* 34: 613–630.

Received for review, May 24, 2013
Accepted, October 29, 2013